411
CT IMAGE SEGMENTATION AND REGISTRATION TO MONITOR DISEASES AROUND THE KNEE JOINT

N. June[1], S. Li[1], X. Cui[1], K-S. Kwack[2], B-H. Min[3], H. Kim[1]. *[1]Sch. of Information and Communication Engineering, INHA Univ., INCHEON, Korea, Republic of; [2]Dept. of Radiology, Ajou Univ. Sch. of Med., SUWON, Korea, Republic of; [3]Dept. of Orthopaedic Surgery, Ajou Univ. Sch. of Med., SUWON, Korea, Republic of*

Purpose: Early diagnosis of OA (osteoarthritis) and monitoring treatment response are very important for OA patients. The follow-up examinations are frequently used by CT scan or MR imaging. The comparison of each medical image from different follow-up examinations is very important for OA treatment. For this comparison, accurate registration of 3D medical images between different CT examinations of same patient should be important to overcome unexpected misregistrations originated from many causes, different patient posture, different field of view, and different resolution of images on each CT scanning. In this study we attempt to show our new fast and effective registration algorithm for medical images.
Methods: A dataset of knee CT images are used to validate a hybrid segmentation and registration method. The CT data is nearly isotropic and the physical size of voxel is 0.36 x 0.36 x 0.5 mm. The fully automatic segmentation based on Active Contour is employed to extract bone regions of knee joint image. Then a two-steps 3D rigid body registration method is performed after segmentation. First, two CT volumes are initially aligned based on their principal axes. Then, the alignment is refined by optimizing the similarity score of the image's voxel. A normalized cross-correlation (NCC) is used as similarity metric and downhill simplex method is employed to attain the optimal score. The registration is separately accomplished for segmented femur and tibia bone region. For each segmented bone volume, new 20 datasets were created by applying random rigid transformation along x-, y-, z-axes varying between ±10 degree for rotation and ±10 pixel for translation.

Table 1. Mean±SD transformation error measurement

	Rotation (°)			Translation (mm)		
	α	β	γ	t_x	t_y	t_z
Femur	0.31±0.44	0.27±0.40	0.28±0.36	0.24±0.15	0.32±0.22	0.18±0.19
Tibia	0.18±0.27	0.06±0.05	0.18±0.13	0.22±0.13	0.32±0.19	0.34±0.34

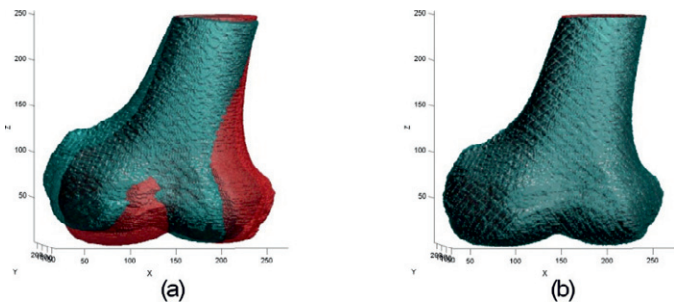

Fig. 1. Femur bone: the superimposed 3D visualization of reference and float volume. (a) before registration, (b) after registration.

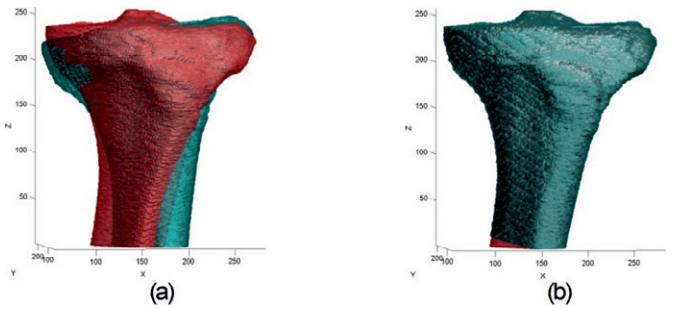

Fig. 2. Tibia bone: the superimposed 3D visualization of reference and float volume. (a) before registration, (b) after registration.

Results: The registration accuracy was 0.21 (±0.26 SD) degrees for rotation and 0.27 (±0.2 SD) mm for translation. The accuracy was evaluated by mean and standard deviation (SD) of transformation errors and rotation errors. Table 1 shows the mean (±SD) of transformation errors and rotation errors of femur and tibia registration. Figure 1 and Figure 2 show 3D visualization before and after registration of femur and tibia bone. Red volume denotes the reference volume and green volume represents float volume. The figures demonstrate that the float volumes were aligned to the same coordinate of reference volumes accurately.
Conclusions: The preliminary study of synthetic datasets showed that the segmentation and registration method can be readily applicable for monitoring the knee joint disease.

412
EARLY SUBCHONDRAL BONE MORPHOMETRIC CHANGES IN OSTEOARTHRITIS: A MICRO-CT STUDY IN THE MURINE JOINT INSTABILITY MODEL

T. Funck-Brentano[1], W. Bouaziz[1], E. Hay[1], V. Geoffroy[1], D. Hannouche[2], M.E. Cohen-Solal[1]. *[1]INSERM U606, PARIS, France; [2]CNRS UMR 7052, PARIS, France*

Purpose: Subchondral bone is involved in osteoarthritis (OA) both at early and late stages. Subchondral bone modifications have been described in mice models of osteoarthritis at early and late stages. However, time-dependent effects of changes in subchondral and trabecular bone are poorly known. The objective of this study is to analyse the changes of trabecular bone structure along with subchondral plate in OA using the model of joint instability in mice.
Methods: To analyse the effects of instability, partial meniscectomy (MNX) of the medial meniscus was performed on right knees of 10 week-old CD1 mice. A sham operation was performed on controlateral knees. At 4 and 6 weeks, samples were fixed and prepared for ex vivo micro-CT acquisition (pixel size 9 µm, Skyscan® 1172, Kontich, Belgium). Then, knees were decalcified and prepared for cryosections. For each medial compartment, the OARSI OA score (sum of the scores at tibiae and femurs) was the mean of 3 saggital slide levels stained by Safranin-O. Morphometric analyzes by micro-CT were performed in the medial tibial plateau to study the trabecular network. Subchondral plate thickness was also measured on reconstructed images. Wilcoxon's tests were performed.
Results: Animals were sacrificed at week 4 and 6. The OA score confirmed a time-dependent effect of MNX in cartilage degradation (4.00 and 6.22 at 4 and 6 weeks respectively). At week 4, micro-CT showed a marked decrease in bone volume in MNX knees compared to sham (BV/TV: 47.6% ± 5.0 vs 62.0% ± 4.7, respectively) which was still observed at week 6 although milder (51.2% ± 2.9 vs 58.0% ± 1.5, $p = 0.028$). These results were accompanied by a higher trabecular separation markedly more severe at week 4 indicating that bone loss was related to a higher bone resorption. No significant effect on the thickness of subchondral plate was observed at week 4 but a mild increase appeared at week 6 (0.184 mm vs 0.171 mm, $p = 0.043$).
Conclusions: These preliminary results show that micro-CT evaluation of tibial epiphysis trabecular network and subchondral bone plate thickness is a reliable technique in the murine joint instability OA model. This confirms that an initial decrease in bone volume occurs at the early stages of the disease. Further experiments with greater number of animals are required to describe subchondral bone morphometric changes in a time-dependent fashion.

413
CARTILAGE SIGNAL INTENSITY ON MRI: ASSOCIATION WITH BODY MASS INDEX, CARTILAGE DEFECTS AND TYPE II COLLAGEN BREAKDOWN

O. Stannus[1], G. Jones[1], F. Cicuttini[2], C. Ding[1,2]. *[1]Univ. of Tasmania, Hobart, Australia; [2]Monash Univ., Melbourne, Australia*

Purpose: MRI has enabled the observation of many abnormal features of OA. However, the ability of MRI to detect early osteoarthritic changes is limited. Our aim was to develop a semi-automatic computer program to assess cartilage signal intensity on T1-weighted MRI images, and then examine whether signal intensity is associated with 1) body mass index (BMI), 2) cartilage defects, and 3) type II collagen breakdown in young to middle-aged adults.
Methods: A total of 50 subjects (mean age 41, range 29–57; 64% female) were randomly selected from the community. MRI scans of right knees were performed (sagittal T1-weighted fat saturation 3D gradient recall

acquisition in the steady state; flip angle 55°; repetition time 58 ms; echo time 12 ms; 512x512 matrix with 0.31x0.31 mm resolution; 60 partitions at 1.5 mm thickness). Image segmentation was performed semi-automatically using custom software written in MATLAB, and measures of mean signal intensity for different regions of cartilage were obtained. Urinary levels of C-terminal crosslinking telopeptide of type II collagen (U-CTX-II) were measured. Cartilage defects were scored using a 5-point scale. Multivariable linear regression was used to test associations.

Results: Cartilage signal intensity varied by site (mean (SD) for femur: 120.1 (8.4); medial tibia: 94.5 (9.8); lateral tibia: 95.9 (11.6); patella: 123.4 (10.7)). After adjustment for confounders, BMI was negatively associated with mean signal intensity of cartilage in the medial femoral ($\beta = -0.82$ per kg/m^2, $p = 0.005$), lateral femoral ($\beta = -0.69$ per kg/m^2, $p = 0.020$), whole femoral ($\beta = -0.60$ per kg/m^2, $p = 0.034$) and lateral tibial ($\beta = -0.80$ per kg/m^2, $p = 0.027$) sites. Cartilage defects were associated with same-region mean intensity in the lateral tibia ($\beta = -10.22$ per grade, $p = 0.017$), and patella ($\beta = -6.06$ per grade, $p = 0.002$). After excluding cases with cartilage defects, CTX-II was negatively associated with mean signal intensity in the medial femoral ($\beta = -2.46$ per pg/ml, $p = 0.010$), lateral femoral ($\beta = -2.13$ per pg/ml, $p = 0.036$), whole femoral ($\beta = -2.44$ per pg/ml, $p = 0.010$) and patellar ($\beta = -2.77$ per pg/ml, $p = 0.031$) sites.

Conclusions: Reduced cartilage signal intensity on MRI is associated with early osteoarthritic changes and thus may be used as a marker of early osteoarthritis.

414
FINDING DISCRIMINATIVE REGIONS THAT OPTIMALLY SEPARATE HEALTHY AND OSTEOARTHRITIS KNEES

D.R. Jørgensen[1], M. Lillholm[2], E.B. Dam[2]. *[1]Univ. of Copenhagen, Copenhagen Ø, Denmark; [2]BiomedIQ, Rødovre, Denmark*

Purpose: The pathogenesis of osteoarthritis (OA) is complex, likely consisting of systemic, biochemical processes as well as focal, biomechanical effects. Based on knee MRI, we investigated whether specific regions of the articular cartilage were particularly different between healthy and OA knees; providing evidence for OA to be mainly a focal or a global cartilage disease.

Methods: 286 right and left knees from 159 community recruited subjects aged 21 to 81 years were scanned using a Turbo 3D T1 sequence on a 0.18T MRI Esaote scanner. The medial tibial cartilage compartments were segmented. From the segmented cartilage sheets, average thickness was quantified on a 7x15 grid, aligned for anatomical correspondence. The knee radiographs were classsified by a radiologist using the Kellgren-Lawrence (KL) scale (0–4).

The knees were divided in two groups, KL=0 (healthy, 144) and KL > 0 (OA, 142). The reference ability to separate healthy from OA knees based on thickness was evaluated were all regions were equally important and evaluated in terms of required sample size.

A Dynamic Partitioning Framework was used to split the cartilage grid into discriminative regions to optimize the separation of healthy and OA knees and evaluated through the required sample size. This process generates a non-negative importance weight for each of the 105 regions.

Results: The median sample size for the reference experiment was 302. For the optimized weight map, the sample size was 122. The improvement, in terms of required sample size, was significant, $p = 1.4 \times 10^{-18}$.

The optimal weight map highlighted a sub-region in the medial tibial cartilage located in the central, external area.

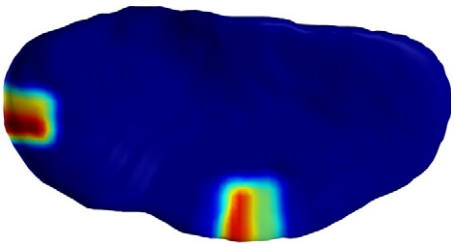

Conclusions: The results demonstrated that there was a focal region providing improved discrimination between healthy and OA knees. The effect in this area could be explained by excess, focal load due to meniscal subluxation and/or varus alignment of the knee. This supports a biomechenically oriented disease progression.Initially, the framework can generate hypotheses for continued research into OA etiology. Eventually, the resulting reductions in sample size could lead to more cost-effective clinical trials.

415
EFFECTS OF SPIN-LOCK TIME SELECTION IN T1RHO RELAXOMETRY

N.F. Klocke, D.R. Thedens, A. Amendola, D.R. Pedersen. *The Univ. of Iowa, Iowa City, IA, USA*

Purpose: Numerous studies have investigated T1ρ relaxation values for cartilage *in vivo*, but the variety in imaging parameters among multiple centers hinders elucidation of the mechanisms underlying T1ρ relaxation changes seen in OA progression. One important parameter in T1ρ imaging is the set of variable spin-lock (SL) times. Objectives: 1) To identify and document the effects of SL time selections on the resulting T1ρ relaxation properties of healthy cartilage at 1.5T and 3.0T fields; 2) To determine the minimal set of SL images necessary to properly ascertain absolute cartilage T1ρ relaxation times.

Methods: After Institutional Review Board approval and subject consent, one healthy 23 year-old female was imaged on the same day in a 3T Siemens TIM Trio scanner and an Avanto 1.5T scanner using a quadrature knee coil with a FSE-based T1ρ acquisition. Twelve SL times at 400 Hz were chosen (SL=0.5, 5, 10, 15, 20, 25, 30, 40, 50, 60, 70, 80 ms) for a 2D oblique sagittal slice through the LFC midline. Other imaging parameters were slice thickness=4 mm, TR/TE=3000/10 ms (3.0T), 3000/12 ms (1.5T), echo train length=13, FOV=140 mm$\times$140 mm, in-plane resolution=0.55 mm. All possible (4017) SL permutations of three or more SL times generated relaxation maps after automated registration of the SL images using a non-linear least squares, mono-exponential fit with a bilinear squares robustness measure applied on a voxel-by-voxel basis using Matlab. A small cartilage ROI (n = 177 voxels for 1.5T images, n = 277 voxels for 3.0T images) was manually selected for analysis in all images (mean, min, max, SD relaxation times reported for each map). Student's two-tailed t-test with equal variance determined statistical significance ($p = 0.05$), to determine similarity to the full-data map made with all 12 SL times. For each number of SL times (3–11), the most similar SL combination was determined in both 3.0T and 1.5T. Another criterion for a "true fit" was normalized means (to the full-data map mean) which were set between 0.975–1.025. The fraction of the maps per SL images within this criterion was also derived. Optimal SL times were determined for each number of SL images to generate equivalent relaxation maps at each field strength. The criteria were that a SL combination's normalized mean signal intensity was within the 0.975–1.025 range, and had the highest pval seen in both 3.0T and 1.5T compared to the other common, high-scoring SL combinations.

Results: For the full-data maps, T1ρ relaxation means ($\pm$SD) were found to be 45.1 ($\pm$8.4) ms at 3.0T, and 46.9 ($\pm$7.6) ms at 1.5T in the defined ROI. Reduced sets of SL times increased the magnitude and spread of T1ρ relaxation times. As the number of utilized SL times increased, the count of SL permutations within the normalized mean criterion increased (3.0T: 8.2% at 3SL to 91.7% at 11SL, 1.5T: 15.9% at 3SL to 91.7% at 11SL). Pvals for the highest scoring SL times on the 1.5T system were between 0.9744 (3 SL combination) and 1.0000 (10 SL combination), and at 3.0T these were between 0.9201 (3 SL combination) to 0.9984 (7 SL combination). The top three optimal SL combinations across fields which had the highest pval scores on both systems came from 4 SL=5, 25, 30, 80 ms (3.0T pval: 0.9631, 1.5T pval:0.9985), 7 SL=0.5, 5, 15, 25, 40, 70, 80 ms (3.0T pval: 0.9704, 1.5T pval:0.9922), and 9 SL= 0.5, 5, 15, 20, 30, 40, 50, 70, 80 ms (3.0T pval: 0.9842, 1.5T pval:0.9857).

Conclusions: The results of this *in vivo* study demonstrate the importance of careful selection of suitable SL permutations for T1ρ within and across field strengths for consistent measurements. While this study has limitations (single subject), it suggests that image-based non-invasive characterization of cartilage on a routine clinical basis across platforms and field strength requires optimization of the tradeoff between scan time (small number of SL times) and accuracy (larger number) to produce consistent and accurate relaxation values. Both the number of and duration of SL times affected measured T1ρ cartilage values in both 1.5T and 3.0T MRI scanners. This study highlights the importance of using a carefully selected set of consistent parameters across platforms to capture reliable T1ρ measurements for eventual translation into clinical practice.

Funded by NIH NIAMS Program Grant P50 AR055533.